Received: 21 February 2024 | Revised: 28 August 2024 | Accepted: 16 September 2024

DOI: 10.1111/ejss.13587

RESEARCH ARTICLE

European Journal of Soil Science WILEY

Spruce and pine utilization of phosphorus in soil amended with ^{33}P-labelled hydroxylapatite

Louise Rütting[1] | **Diana Hofmann**[2] | **Thomas Pütz**[2] | **Matthias Konrad-Schmolke**[3] | **Roland Bol**[2]

[1]Soil and Plant Systems, Brandenburg Technological University Cottbus-Senftenberg, Cottbus, Germany

[2]IBG-3: Agrosphäre, Forschungszentrum Jülich GmbH, Jülich, Germany

[3]Department of Earth Sciences, University of Gothenburg, Gothenburg, Sweden

Correspondence
Louise Rütting, Soil and Plant Systems, Brandenburg Technological University Cottbus-Senftenberg, Cottbus, Germany.
Email: louise.ruetting@b-tu.de

Abstract

Mined rock phosphate is expected to become a scarce resource within the next few decades as global phosphorus (P) deposits are declining. As a result, mineral P fertilizer will be less available and more expensive. Therefore, improved knowledge is needed on other P resources, for example, apatite fertilizers derived from the by-products of iron mining. Forestry is a potential future consumer of apatite-rich products with the aim of obtaining more wood per hectare. The actual P availability in apatite to plants has so far been barely quantified. We therefore examined tree P uptake using ^{33}P apatite under chamber-grown and outdoor conditions. We examined the P uptake for the two main conifer species spruce (*Picea abies*) and pine (*Pinus sylvestris*) used in Fenno-Scandinavian forestry. We synthesized ^{33}P-enriched apatite and applied it to mesocosms with growing seedlings of spruce and pine. The P uptake from ^{33}P-labelled hydroxylapatite was subsequently traced by (bio)imaging of radioactivity in the plants and by liquid scintillation counting (LSC) upon destructive harvest in all plant fractions (leaves, stem and roots) and rhizosphere soil. Two climatic conditions were compared, one at natural outdoor conditions and one set as 5°C warmer than the climate record from the previous years. Plant P uptake from ^{33}P-labelled hydroxylapatite was enhanced in chamber-grown compared with outdoor seedlings for both tree species. This uptake was manifested in the clear radioactive images obtained over ca. 1 month after soil apatite application. Furthermore, all aboveground plant fractions of both spruce and pine seedlings showed a higher P uptake in warmer than colder daytime environments. The observed quantities and rates of P uptake from ^{33}P-labelled hydroxylapatite by spruce (18 Bq g^{-1} hour^{-1}) and pine (83 Bq g^{-1} hour^{-1}; averages in chamber condition) are as to our knowledge unique observations. Natural forest soils in Sweden are often P-poor. Our research suggests that apatite-based P fertilization of spruce and pine forests can increase wood production by overcoming any existing P limitation.

KEYWORDS
conifer forest, fertilizer, phosphorus resource, Swedish forestry

1 | INTRODUCTION

1.1 | Phosphorus fertilizer

Phosphorus (P) has become a non-renewable fertilizer resource and is becoming less available (Faradji & de Boer, 2016). P mining is predicted to peak in the year 2033 and will thereafter decline (Cordell & White, 2011). Therefore, there is a global interest in finding new P resources and improving industrial-scale recycling of P. Food production systems will then start lacking P as fertilizer will be increasingly unavailable or expensive. Also, P availability in natural ecosystems and managed forests will become an issue, partly because the vegetation may become more P demanding under increased growth in response to global change factors (Zhao et al., 2023). In organic soils, global change effects, such as increasing surface temperatures and increased rainfall, might stimulate organic P mineralization and weathering of minerals, increasing P availability (Hou et al., 2018). For example, P availability increased in a peatland in a long-term warming experiment (Iversen et al., 2023). Furthermore, increased P mineralization was found in CO_2 exposed (FACE) soils (Hasegawa et al., 2016; Yu et al., 2023). However, such increased P availability from natural soil sources cannot meet the needs of forest managers for timber production on upland soils, which is why P fertilization is likely to become necessary (Ståhl & Bergh, 2013; Magnusson, 2015).

1.2 | Spruce and pine in Swedish forestry

Within Sweden, the land area of 40.7 M ha includes 23.5 M ha of production forest, whereof 9.5 M ha is pine and 6.4 M ha is spruce (SLU Forest Statistics, 2023). Limiting nutrients, such as phosphorus (P) and nitrogen (N), are of high interest. In southern Sweden, annual P losses from forestry exceed 1 kg P ha^{-1} (Akselsson et al., 2008). The soil total P stock was on average only 4.0 $g{\cdot}m^2$ in the Oe horizon, 9.5 $g{\cdot}m^2$ in the A and E horizons, and increased with depth to significantly higher values (117.5 and 109.3 $g{\cdot}m^2$) in the B and C horizons down to 80 cm depth (Tuyishime et al., 2022). Therefore, a limitation of tree growth by P is likely, and it is especially pronounced in South-West Sweden, indirectly caused both by the N deposition gradient (He et al., 2021; Yu et al., 2018) and soil acidity (SLU Mark och Miljö, 2023). Forest fertilization in Sweden was abundant in the 1970 due to high demand for timber (Jacobsen et al., 2005). Here in the 21st century, the fertilization with 150 kg $N{\cdot}ha^{-1}$ is recommended by the Swedish forest agency (Högberg et al., 2014) and its effects can last for 7 to 11 years, resulting in 13–20 m^3 of additional wood biomass growth (Jacobsen et al., 2005). By law, a maximum of 200 $kg{\cdot}ha^{-1}$ mineral N fertilizer is allowed (Skogsstyrelsen, 2015). Conventional mineral fertilizer is commonly used, but also ash (unspecified composition) is used as fertilizer in Swedish forests. The recommended minimal content of P in ash used for fertilization is 7 g $P{\cdot}kg^{-1}$ (Drott et al., 2019), much less than the minimal recommendation for P addition by mineral fertilizers of 40 $kg{\cdot}ha^{-1}$. However, there are no recommended maximum limits by law for P amendment, but individual assessment is given by the authority (Skogsstyrelsen, 2015). Successful field scale fertilization experiments with mineral fertilizers containing 10 to 30 kg $P{\cdot}ha^{-1}$ were set up for optimal spruce leaf N to P ratio (Clarholm & Rosengren-Brinck, 1995; Linder, 1995), but also more intense fertilizations up to 160 kg $P{\cdot}ha^{-1}$ have been tested in the past (Wallander & Thelin, 2008).

Highlights

- Mining products may contain P-rich minerals, but the bio-availability of apatite is barely known.
- Mineral P fertilizer is an increasingly limited resource; new P resources need to be explored.
- By applying synthesized ^{33}P-enriched apatite in mesocosms, we prove pine and spruce uptake by radioactivity.
- Apatite fertilization of spruce and pine forests is feasible.

1.3 | Apatite as fertilizer

Natural apatite ($Ca_5(PO_4)_3$ (F, CL, OH)) is the most abundant group of primary minerals in most soils. In fact, natural apatite is the primary source of all mineral P (Rakovan & Scovil, 2021; Smeck, 1985). Apatite becomes more easily dissolved in increasingly acidic soils, as it undergoes carbonation weathering, releasing phosphate

(Weirauch & Opp, 2018), which is readily available for plant uptake. Biological activity in the soil (plant roots and soil microbes) keeps soil CO_2 levels high, which also increases carbonation weathering due to the slight acidification (Schlesinger & Bernhardt, 2020). As soils in Sweden are considered acidic with pH ranging between 4.5 and 6 in the B horizon and even lower in the O horizon (SLU Mark och Miljö, 2023), phosphate release from apatite is indeed expected (Guidry & Mackenzie, 2000; Wolff et al., 2020). In addition, warmer temperatures can increase soil biological activity (Pendall et al., 2004), indirectly accelerating carbonation and phosphate release from apatite as well. Most Swedish soils were formed after the last glaciation and developed in glacial till and glaciofluvial or wave-washed sand (Adediran et al., 2022). Here, apatite can be hard to observe (Casetou-Gustafson et al., 2019), as the apatite grains are micron-sized (Adediran et al., 2022). Apatite can also be preserved as inclusions in other minerals (Adediran et al., 2022). Therefore, bio-available apatite is lower than the actual abundance of apatite.

A recent recommendation in Sweden is therefore to apply crushed apatite to the forest floor as a P fertilizer product (Ståhl & Bergh, 2013; Magnusson, 2015). Indeed, pot experiments have shown better P content and growth of *Pinus sylvestris* seedlings growing with apatite amendment (Wallander, 2000). In such experiments, production of the weak organic acid oxalic acid (from roots and/or microbes in the soil) was observed and suggested to be a mediator of release of phosphate from apatite (Wallander, 2000; Wallander et al., 2003). However, to our knowledge, no field scale experiments with granulated apatite application have been carried out in Sweden. Mesh-bag experiments have investigated the effect of fertilizer on ectomycorrhizal (ECM) growth and community (Almeida et al., 2019; Rosenstock et al., 2016), and demonstrated that apatite stimulates ECM (Smits et al., 2014; Wallander & Thelin, 2008).

Recently, commercial 'new-phosphorus-fertilizers' are being developed to fulfil requirements of slow release of P in order to minimize the leakage of P to the environment, especially to streams and lakes (Solanki et al., 2015). Examples being tested in agricultural research include nano-sized particles containing a combination of urea and apatite (Kottegoda et al., 2017), and nano-sized hydroxylapatite (Taşkın et al., 2018). As apatite is one of the main waste products from iron-ore mining activities in Sweden, its use is already being explored (EAGE news, 2017).

1.4 | Plant uptake of nutrients

Soil warming might increase plant nutrient acquisition by enhancing root uptake kinetics (Andresen et al., 2009; Basirirad, 2000). According to growth demand, the plant acquires inorganic nutrients such as NO_3^-, NH_4^+ and PO_4^{3-} from the soil solution, while these nutrient ions passively approach the rhizosphere by diffusion and bulk flow as well as from exchangeable cations from soil colloids (Cronan, 2018). This flow supplies the active transport across the plant root plasma membrane and plasmalemma. However, in natural forest soils, the plant root uptake of the soil nutrients is mediated through initial uptake by mycorrhizal hyphae (Becquer et al., 2019; Cairney, 2011; Kumar & Atri, 2017). This can be as a direct uptake of an organic P-rich molecule, or after hydrolytic liberation of inorganic P (P_i) from the organic P via phosphatases exuded by the mycorrhizal roots (Rennenberg & Herschbach, 2013). Indeed, organic bound P is in some cases the largest source of P_i in soils (Roberts et al., 2015). The P_i uptake is aided by transporter proteins in the cellular membranes that also maintain the charge balance through the proton pump (Smith et al., 2002). Once transferred across the membranes, phosphate is transported inside the plant stele by xylem flow and re-translocation transport in the phloem occurs also as phosphates (Bloom et al., 1985). The governing hypothesis is that ECM and saprotrophic fungi mine the minerals in soil directly and give the nutrients to the plants in mutualist exchange for carbohydrate supply (Colin et al., 2021; Smits et al., 2012). Indeed, spruce uptake of P by ECM fungi was regulated by the photosynthetic carbon supply to the fungi (Bucking & Heyser, 2003).

Alongside the development of modern P-rich fertilizers, it has been discovered that plants can take up nutrients from nanoparticles and incorporate the elements into the plant biomass (Rico et al., 2011). The uptake of nanoparticles into plant cells happens through the pores of the cell wall and thus depends on the pore diameter which is usually in the order of 5–20 nm. However, synthetic nanoparticles can be designed to enlarge the pore size or induce production pores (Solanki et al., 2015). Furthermore, nanoparticles can bind to carrier proteins through aquaporin, ion channels or end inside the cell after endocytosis where the plasma membrane forms a cavity around the particle and releases it inwards (Nair et al., 2010). In fertilization experiments with spherical nanoparticles of 16 ± 7 nm diameter pure hydroxylapatite, soybean plant biomass benefited (Liu & Lal, 2014). Likewise, maize plants (angiosperms) benefitted from nano-sized rock phosphate particles (Adhikari et al., 2014). However, to our knowledge, no experiments have investigated spruce and pine uptake of nanoparticles, although uptake of apatite in form of nanoparticles is hypothetically possible by these gymnosperms as well.

1.5 | Experimental design and aims

Our experiment was designed with the aim to prove the uptake of ^{33}P-enriched apatite by spruce and pine seedlings from Swedish forestry at a level of P fertilization similar to conventional forest P fertilization intensity. Hence, we simulated conventional forest fertilization with 13 kg P ha^{-1} in the laboratory experiment by using rhizotrons (fixed plant boxes) with hand-packed soil. ^{33}P-enriched apatite was used in the soil to avoid undesired exposure of the aboveground plant to ^{33}P-induced radioactivity from the surface. The experimental work with radioactivity had some practical limitations given by safety considerations (ALARA principle—As Low As Reasonably Achievable), as no unnecessary exposure of the radioactive label was desirable. Hence, the ^{33}P-enriched apatite was applied deeper inside the soil and not at the ground surface to prevent release of radioactive dust, which contrasts to normal forest fertilization where the fertilizer would be spread out on the surface. Furthermore, a main experiment with many replicates, with a usage of a minimum amount of radioactive label (total 4 mCi) was decided upon after completion of two pilot experiments with single plants (using 1 mCi each; data not shown).

Our hypotheses were that: (i) we would observe fast uptake of ^{33}P-apatite in both conifer species, observable using (bio)imaging and scintillation counting of plant material extracts; and (ii) chamber-grown plants have faster needle ^{33}P-uptake rate than under outdoor conditions.

2 | MATERIALS AND METHODS

2.1 | Pine and spruce seedlings

The experimental plants were two species: pine *Pinus sylvestris* of the provenience Asarum (FP611 S16/008), provided as seeds, and spruce *Picea abies* of the Bredinge type (FP501 S12/68) from 'Södra Skogsplantor' in Sweden.

Pine seeds were sown indoors in pots with soil from a natural spruce forest at the end of March 2021, growing outside from May until the experiment took place in fall and winter 2021. The seedlings were 6 months old at the time of the experiment. Spruce seedlings were bought in June 2021, after frozen storage with Cambiguard (Södra Forest; physical protection against pests; Domevscik et al., 2024), being 2 years old at the time of the experiment. All spruce and pine were re-potted into a soil mix of commercial unfertilized peat soil (Naturtorv, Solmull, Sweden), quartz sand (Quarzwerke) and commercial soil (standardized substrate type 0; Einheitserde, Einheitserdewerke Werkverband e.V., Germany). This mix was inoculated wet with a spike of spruce forest topsoil for a natural microflora. By late September 2021, the seedlings were transplanted into self-made standardized mini-rhizotrons (boxes that can be opened, according to Hofmann et al., 2023; Schreider et al., 2022). Pine rhizotron dimensions were 12 × 12 × 1.5 cm adapted from square petri dishes together with thin office transparencies that were glued watertight with heated glue. Spruce rhizotron dimensions were 52 × 35 × 4 cm, constructed from PVC plates (Bauke et al., 2017; Wolff et al., 2020). The one removable side was sealed with a rubber gasket and screwed on. All rhizotrons were tilted at a 45° angle to force roots to grow along the removable side of the rhizotron (Figure 1). Plant and soil dry weights were obtained after drying at 50°C. Start conditions in plant and soil parameters and element contents are given in Table S1.

2.2 | Growth conditions

The seedlings grew from 17 September 2021 to 1 March 2022 in two parallel sets, one set at outdoor conditions and one set in a climate chamber at planned elevated temperatures (each 7 pine and 10 spruce). The chamber was planned to be 5°C warmer than outdoors, by using the previous year's weather records. Daylength (light intensity of 670 µmol, light sensor reader: Fieldscout, Spectrum Technologies, USA) was kept as outside (20–1030 µmol; Table S2). The climate chamber was a CLF Plant Climatics, Percival (Germany), from 2009 (2 m × 1.45 m × 75 cm) placed in the radioactive control area of IBG-3 at Forschungszentrum (FZ) Jülich. All rhizotrons were watered weekly while keeping initially the total soil moisture at 60% water saturation. During the last weeks with radioactive label, watering was kept at a minimum 1–2 days before bio-imaging to avoid bad image quality. A P-free fertilizer mixture was mixed from: KNO_3, $Ca(NO_3)_2$*$4H_2O$, $MgSO_4$*$7H_2O$ (Table S2).

2.3 | Elemental analysis of plant and soil

At the onset of the experiment, selected plants were harvested for the analysis of initial contents of N, P, Mg, Ca and K. The dried spruce and pine material was divided into needles, stem and roots (>2 mm thick). The plant materials as well as a soil sample were powdered using a Retsch mill. A total of 50 mg of each sample was digested with 250 mg Lithiumborat for 1 h at 1050°C. After cooling the digest, 50 mL 5% HCl was added, and this

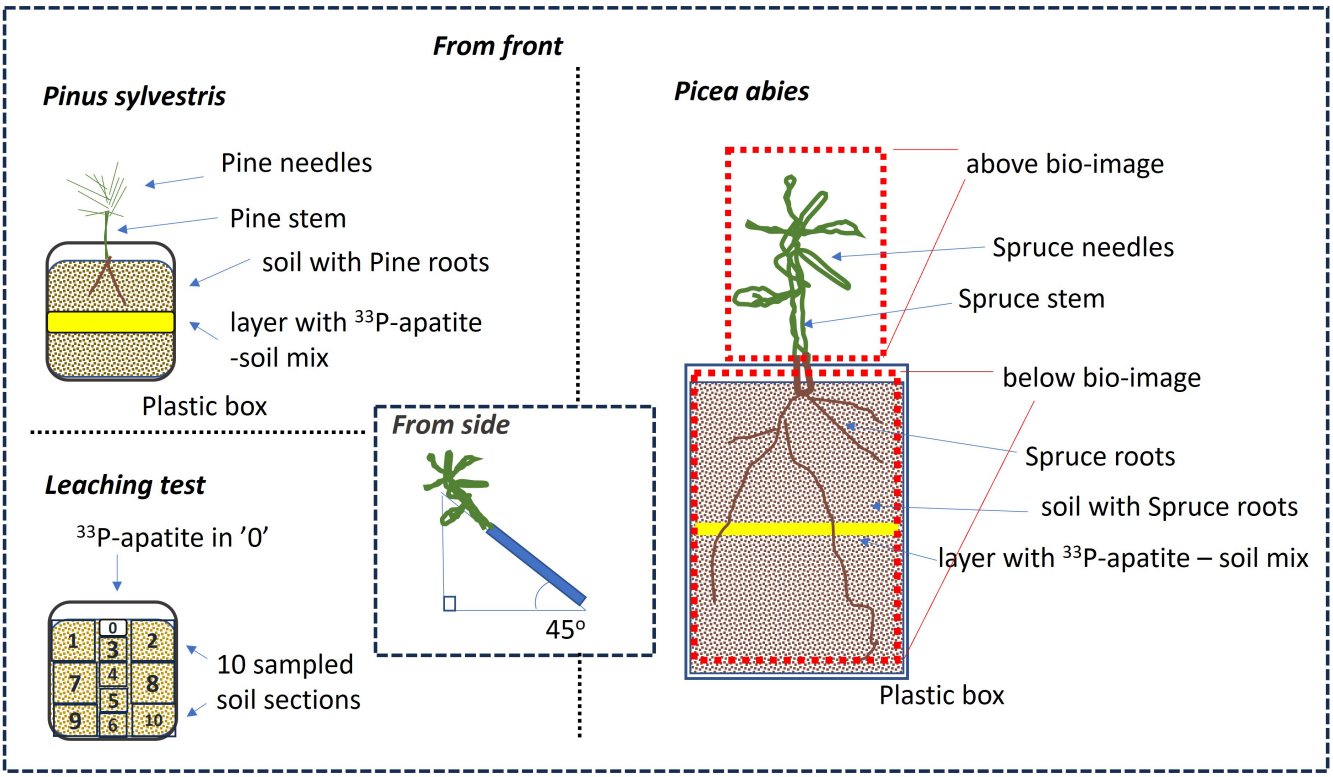

FIGURE 1 Design of growth systems for pine (*Pinus sylvestris*) and spruce (*Picea abies*). Front-view diagram of the pine (*P. sylvestris*) rhizotrons and the spruce (*P. abies*) rhizotrons. Side-view showing how both rhizotron types are tilted 45° during growth. Yellow band indicates the placement of the ^{33}P-enriched apatite-soil layer. The red stippled frames indicate the placement of bio-image plates for spruce; for pine, the entire plant and rhizotron was captured by one (bio)image plate. At the end, the plants were separated into the components: Leaves (needles; green), stem (green), woody roots (brown) and fine roots (thin brown) for digestion and LSC analysis. A leaching test was made with ^{33}P-enriched apatite (white layer 0) in a similar plastic box as for pine. After 4 weeks, the soil in the plastic box was sectioned into 10 separate samples, and each was digested for LSC analysis (Figure S5).

digestate was analysed for total P, Mg, Ca and K with 2 analytical replicates utilizing a ICP-OES (iCAP7600, Thermo Scientific) at ZEA-3 within FZ Jülich. Furthermore, 5 mg of each sample powder was analysed with 3 analytical replicates with an elemental analyser (varioELcube, Elementar, Langenselbold, Germany) for total C and N (Table S1). Soil pH was 4.4.

2.4 | Production of radioactive apatite

The ^{33}P-labelled hydroxylapatite was uniquely synthetized in a three-step procedure at ambient room temperature inside a fume hood in the control area of IBG3 FZ Jülich through 2 days before the application of the label to the mini-rhizotrons. We used 4 mCi of ^{33}P-orthophosphate (Hartmann Analytic, Braunschweig, Germany) to obtain a yield of 8.5 g blended ^{33}P-hydroxylapatite by the following procedure. First, 4 M HNO_3 was added dropwise to a 2 M CaO suspension reaching a pH of 1.5. In parallel, a 25% phosphoric acid solution, containing the entire ^{33}P purchase, was added dropwise to a 25% NH_3 solution. Then, these $Ca(NO_3)_2$ and $(NH_4)_2HPO_4$ solutions were brought together to react under pH 9–10 with addition of Ethanolamine (3 wt%) to avoid aggregation. After 12 h stirring, the reaction product was filtered and washed several times with water and subsequently with absolute ethanol. The product was dried overnight in a drying cabinet at 50°C and then underwent calcination at 200°C for 2 h, forming hydroxylapatite (for more details see Wolff et al., 2018; Hofmann et al., 2023). We achieved a synthesis efficiency for ^{33}P of 78%.

2.5 | Scanning electron microscopy and EDX analyses

Backscattered electron (BSE) images and chemical analyses of the natural and synthetized apatite samples were generated using a Hitachi S-3400 N scanning electron microscope (SEM) equipped with an Oxford Instruments X-Max energy dispersive spectrometer at Department of

Earth Sciences at the University of Gothenburg, Sweden. Operating conditions involved a 20 kV acceleration voltage and a beam current of 6 nA. The instrument was calibrated on a cobalt standard, and the integrated counting time was 40 s for each analysis. Analytical errors, that is, 2σ reproducibility on major and minor elements, under these operating conditions were about 5% relative to the mean (Roeder et al., 1987; Figure S1).

2.6 | Raman spectroscopy

Laser-induced Raman measurements were carried out at room temperature using a Horiba (Jobin Yvon) LabRam HR Evolution at Department of Earth Sciences at the University of Gothenburg, Sweden. The samples were excited with an air-cooled frequency-doubled 532 nm Nd-YAG laser utilizing an Olympus 10× objective. The lateral resolution of the unpolarized confocal laser beam was on the order of 1 μm. Spectra were generated in the range of 50 to 4000 cm^{-1} utilizing an 1800 grooves/cm grating and a thermoelectric cooling electron multiplier CCD including a front illuminated 1600 × 200 pixel chip. The spectral resolution on the unoriented sample was in the order of 1 cm^{-1}. The wavenumber calibration was done using the 520 cm^{-1} Raman band on a polished silicon wafer with a wavenumber accuracy usually better than 0.5 cm^{-1}. Raman spectra of the samples were collected through 2 acquisition cycles with single counting times of 30 s (Xu et al., 2020; Figures S1A and S1B).

2.7 | ^{33}P-apatite application to the mini-rhizotrons

The 8.5 g blended apatite was ground to powder in an agate mortar and mixed subsequently with 1.1 kg air dry soil in a plastic bottle, placed inside a closed barrel of a drum hop mixer (Rhönradmischer RRM ELTE 650, Engelsmann, Ludwigshafen, Germany) at 10 rpm for 4 h. The ^{33}P-apatite-labelled soil contained 0.115 MBq per g soil, corresponding to 8.474 mg apatite per gram soil (0.26 mg P per gram soil). It was divided into portions of 5 g soil (containing 0.5755 MBq in 42 mg apatite with 1.3 mg P) for the pine rhizotrons and 50 g soil (containing 5.755 MBq in 424 mg apatite with 13 mg P) for the spruce rhizotrons. In the pine rhizotrons, the ^{33}P-labelled soil was added to the soil at a depth of 6–8 cm (Figure 1) by replacing the packed soil and gently pushing the labelled soil into the 'ditch' with a porcelain rod. The rhizotrons were covered with light-tight black plastic. In the spruce rhizotrons, the ditch in the packed soil was in 20 cm depth (Figure 1). Roots were carefully moved to the side while adding the labelled soil, and roots and a bit of 'cold', that is, non-radioactive, soil was laid over the labelled band before closing the boxes plastic lid tightly with screws.

2.8 | (Bio)imaging via digital autoradiography

All rhizotrons were monitored weekly: the rhizotrons were laid on a table and the cover plates carefully removed to reach the soil surface. Phosphor imaging plates containing Europium complexes (DÜRR NDT GmbH, Bietigheim-Bissingen, Germany) were wrapped in thin protection foils and subsequently placed on the entire rhizotron (pine) including aboveground and belowground plant parts or separately on the root overgrown peat soil and on the aboveground plant (spruce). During an exposure in complete darkness, a gentle weight on top of the imager plates ensured the best contact between the plants/rhizotrons and the imaging plates. Two pilot plants were exposed for 4 h, while in the main experiment (with lower ^{33}P amount), we used 6 h exposure time. With the rhizotron, we incubated a standard series of ^{14}C polymer references with six different activities 66, 223, 692, 1867, 7067 and 18450 Bq cm^{-2}, each covering a surface area of 1 cm^2 (IPcal test source array; ELYSIA-Raytest, Straubenhardt, Germany). The plates were scanned in complete darkness using a plate scanner (Bioimager CR35 Bio, Raytest, Straubenhardt, Germany) in sensitivity mode at a resolution of 100 μm, which releases light at 390 nm by the helium laser ablation at 633 nm (Koch et al., 2019). Before each image, the plates were double erased by a light imaging plate eraser (Fujifilm, Tokyo, Japan) followed by erasing with the (bio)imager CR35 Bio (ELYSIA-Raytest, Straubenhardt, Germany). Digital images were further processed with the evaluation software AIDA (AIDA Image Analyser 2D densitometry program, Raytest, Straubenhardt, Germany). For comparability, all images were presented in rainbow mode using 1.8 as optimized amplification factor.

2.9 | Harvest of ^{33}P-plant material from mini-rhizotrons

The aboveground plant was cut at the soil surface and divided into needles and stem material. For pine rhizotrons, first in the belowground soil, a subsample of bulk soil was taken far from visible roots. The plant was lifted and lightly shaken; thereby, rhizosphere soil was

sampled from the soil adhering to the roots. Hereafter, roots were washed to remove any soil. For the spruce rhizotrons, three belowground layers were kept separate, one layer below the apatite layer (bottom soil) and two layers above the apatite layer (top and middle soil). From each of the three layers, bulk soil was sampled. Following this, the plant was lifted out and rhizosphere soil was sampled as soil adhering with the roots (all depths combined). Roots were cut into the three layers. All plant material and soil samples were dried at 50°C for 1–2 days until weight constancy.

2.10 | Sample digestion and liquid scintillation counting

Sub-samples of soil and plant material (max 0.5 g each), respectively, were covered with 4 mL 65% HNO_3 in a closed Teflon container and heated under pressure for 6 h at 180°C (Loftfields Analytische Lösungen, Neu Eichenberg, Germany). These digests were diluted with 25 mL MilliQ water and filtered. 1 mL of each sample was manually shaken with 10 mL Ultima Gold XR (PerkinELmer, Waltham, MA/ USA) and after resting for an hour, counted for radioactivity at a scintillation counter (liquid scintillation counting (LSC); TriCarb 3110TR PerkinElmer, Waltham, MA/ USA) through 60 minutes (Hofmann et al., 2023).

2.11 | Leaching tests

In order to test if apatite-P could leach and spread through the soil system, a test was made in a separate setup in a similar plastic box as for pine rhizotrons (Figures 1 and S5). (Bio)imaging (as above) was made once per week to follow any visible spreading of radioactivity. Finally, soil was separated after 30 days into 10 sections, digested and analysed by LSC (Figure S5).

As a further test of apatite solubility leading to Ca and P leaching in the soil, three samples of 30 g air dried soil were prepared: (i) mixed with 1 g apatite (28.2 (± 1) % Ca, 15.4 (± 0.3) % P), having a soil pH of 5.6 after extraction; (ii) mixed with 1 g NPK fertilizer (3.65 (± 0.05) % Ca, 5.48 (± 0.11) % P) plus 200 mg $CaCl_2$, having a soil pH of 5.6; and (iii) same soil as control without any additive, having a soil pH of 5.1. 100 mL MilliQ water was added, and after a rigorous shaking, the samples stood for 24 h. Then, soils were filtered through 0.45 µm filter, pH was measured and ICP-OES (iCAP 7600) of the extracts for Ca and P content (double analysis) was performed (Table S4).

2.12 | Calculations of P uptake from ^{33}P-labelled hydroxylapatite

All LSC values were first decay-corrected (Schreider et al., 2022). The total amount ^{33}P-apatite plant uptake was calculated as the sum of ^{33}P concentrations (Bq per gram dry weight) multiplied by the biomasses (gram dry weight) within each plant fraction (needle, stem, root). The recovery of ^{33}P-apatite label was calculated as the total amount ^{33}P-apatite plant uptake relative to the total amount ^{33}P-apatite added to the rhizotrons (0.575 MBq in the pine rhizotrons and 5.755 MBq in the spruce rhizotrons).

2.13 | Statistical analysis

For testing effect of treatment ('chamber' vs. 'outdoor') on absolute radioactivity data (µCi g^{-1}), within species and the same number of days for uptake, we used a paired *t*-test (being paired by the harvest date) for normal distributed data (Shapiro–Wilk) and a Wilcoxon signed-rank test for not-normally distributed data, indicating a significant difference when p value <0.05.

3 | RESULTS

Uptake of the ^{33}P hydroxylapatite amendment was detected after 3 or 4 days with the (bio)imaging (Figures 1 and 2). The time series of the (bio)images described a continuous increase of radioactivity over the experimental period (up to 42 days). Remarkably, this could be observed despite the decay of ^{33}P (half-life of 25.4 days). Furthermore, there was a significant difference in ^{33}P-based radioactivity in the (bio)images between the outdoor and chamber-grown plants, with a weaker signal in outdoor grown, especially for spruce (Figures 1 and 2).

There were also significant differences of chamber vs. outdoor grown plant material in LSC analysed digests of pine needles (e.g. leaves, $p = 0.004$; $n = 7$ & 7; paired *t*-test) and pine stem ($p = 0.016$) and of spruce needles ($p = 0.0002$; $n = 8$ & 8; paired *t*-test), spruce stem ($p = 0.0005$), spruce roots ($p = 0.0113$) and spruce rhizosphere soil ($p = 0.049$). The pine needle uptake rate was on average 83 (± 52) Bq g^{-1} $hour^{-1}$ and 28 (± 24) Bq g^{-1} $hour^{-1}$ for pine grown in chamber and outdoor conditions, respectively. For spruce, the needle uptake rate was on average 18 (± 8) Bq g^{-1} $hour^{-1}$ and 1.5 (± 1.1) Bq g^{-1} $hour^{-1}$ for spruce grown in chamber and outdoor conditions, respectively. The total plant uptake in pine ranged from 2.4 to 6.0 mg apatite (equal to 0.10 to 0.18 mg P), in chamber-grown pine and 0.2 to 2.4 mg

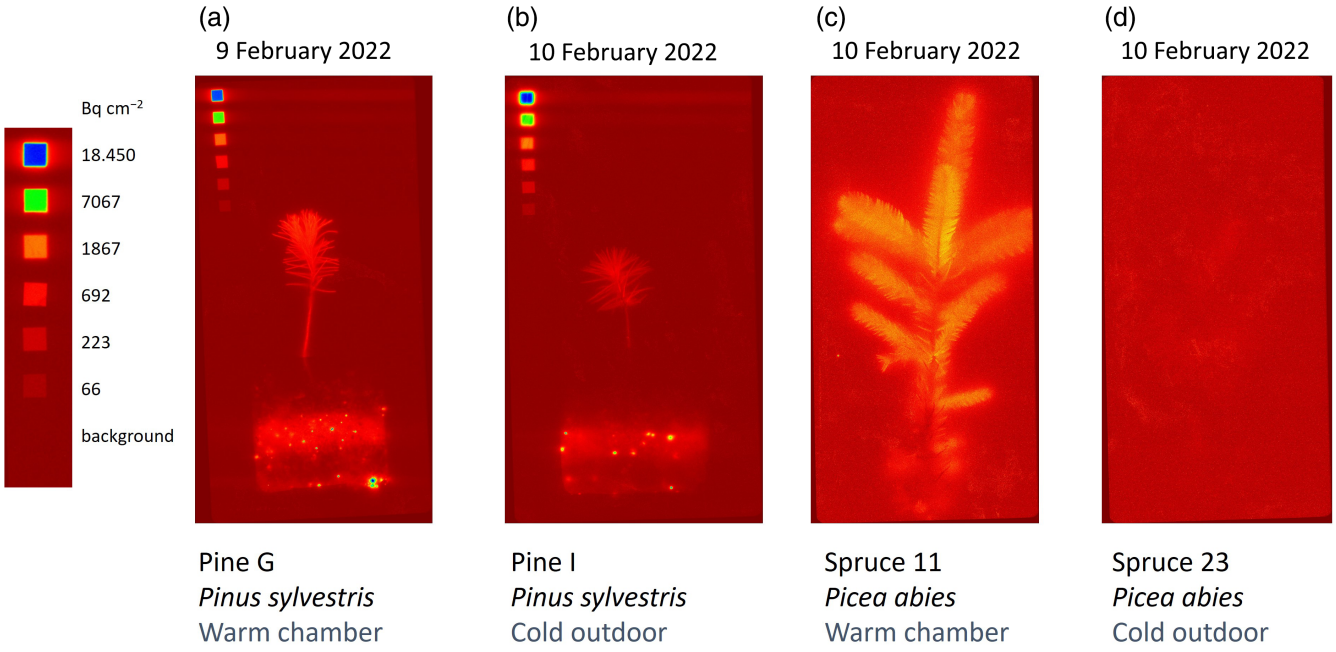

FIGURE 2 (Bio)images of ^{33}P by scanning of beta-radiation-sensitive europium-enriched plates exposed for 6 h to pine (a & b) and spruce (c & d) plants after c. 20 days (date of imagery indicated at top) of root uptake from soil amended ^{33}P-labelled hydroxylapatite (amended on 21 January 2022). The scale on left is a standard series of a ^{14}C polymer references with six different activities. The plants named pine G and spruce 11 were growing in the daytime warm chamber, while the plants pine I and spruce 23 were growing in daytime cold outdoor conditions. See Figure S4 for more (bio)images and time series of pine and spruce plants and diagram of the incubation set up.

apatite (equal to 0.02 to 0.07 mg P) in outdoor grown pine, based on the ^{33}P recovery (Figure S2). The total plant uptake in spruce ranged from 6.4 to 81.3 mg apatite (equal to 0.20 to 2.51 mg P) in chamber-grown spruce and 0.4 to 16.0 mg apatite (equal to 0.01 to 0.49 mg P) in outdoor grown spruce (Figure S2). In spruce, the acquired amount of P was 7%–15% (chamber grown) and 0.1%–3% (outdoor grown) of the total plant P stock; and in pine, the acquired amount of P was 88%–155% (chamber grown) and 13%–61% (outdoor grown).

The low radioactivity found in the rhizosphere soil (Figures 3 and 4) contrasted to the absence of radioactivity in the bulk soil (Figure S3). Furthermore, the apatite leaching test (Figure S5) suggested no significant leaching of apatite-P away from its position, as the soil directly below the ^{33}P-apatite (soil nr. 3, see Figure 1) had after 1 month only 0.59% of the P added with the apatite (towards a standard deviation of 1% in the main part), which likely happened during installation or sampling—laterally even lower with 0.1%. In the (bio) images (Figure S5), neither veils nor hot spots were detected. Much more important, the section below (nr. 4) did not have activity (<0.01%). All more distant soil sections had less than 0.01% of the added P in the apatite.

As a further test of both P and Ca leaching under rigorous shaking, we found that only 1% of the apatite-P and Ca, respectively, were dissolved under these conditions. By contrast, NPK fertilizer as agrochemical additive, formulated for delayed release, showed 4% P release. The even higher 10% Ca release came from our combination of Ca-containing NPK and an easily soluble Ca salt (Table S4).

4 | DISCUSSION

Both conifer species had clear and fast uptake of P from apatite, and both very young and older seedlings had similar comparable P uptake from ^{33}P-labelled hydroxylapatite. Thus, regardless of the exact uptake rates, individual plants of both species showed increasing radioactivity in the time series by (bio)imaging. This suggests continuous uptake despite the fact that the half-life of ^{33}P was exceeded during the uptake experiment. Both spruce and pine seedlings acquired a substantial amount of P from apatite during the experiment, reflecting the nutrient needs and limitations, as all plants were otherwise grown under P starvation. The pine seedlings had a more rapid uptake of P than spruce, which we suggest is due to their young age. To our knowledge, these are the first data of their kind in a laboratory setup with conifer plants and we are not aware of any experiments in the field that determine tree uptake of apatite.

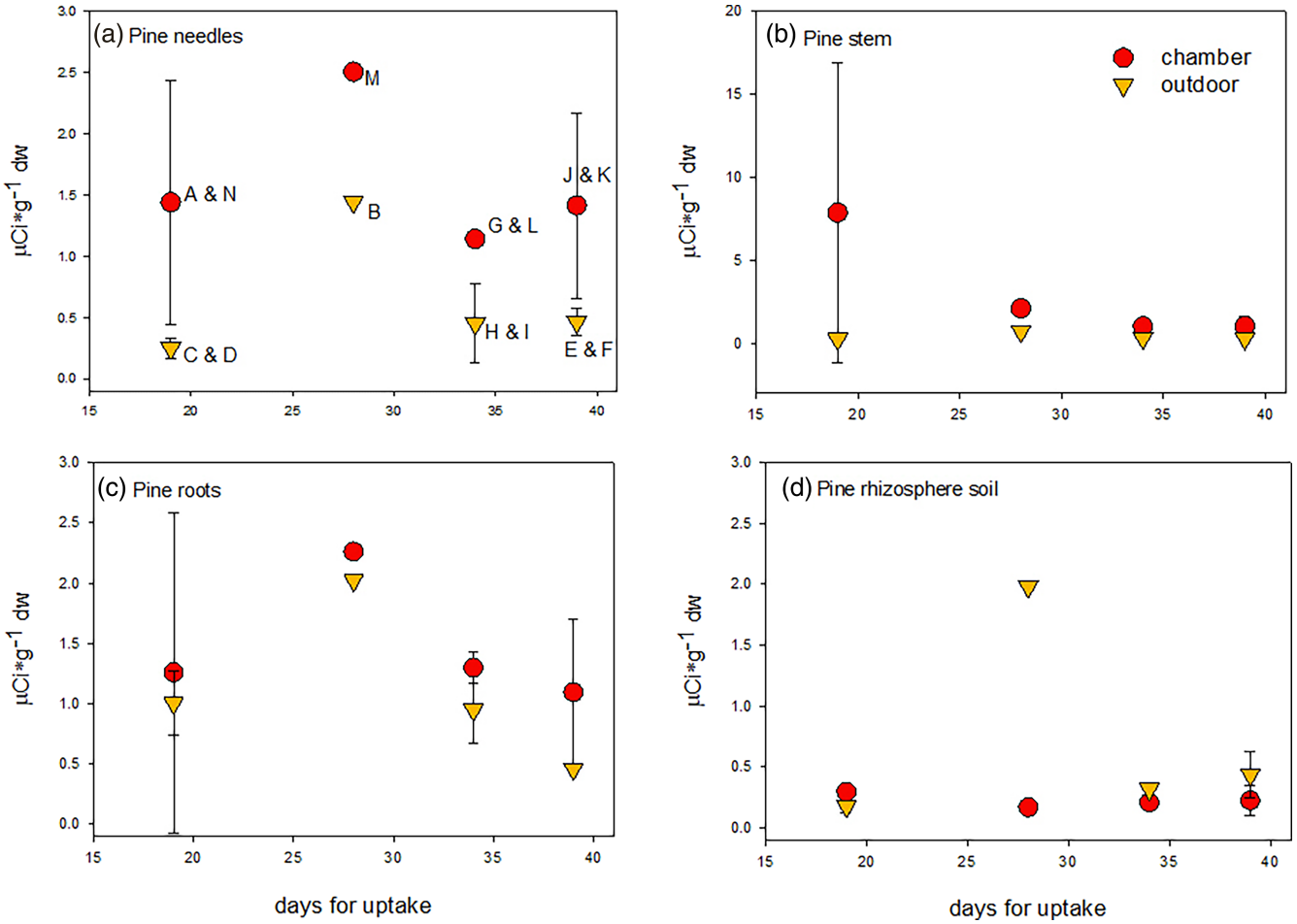

FIGURE 3 Absolute radioactivity as micro-Curie per gram dry weight (dw) after harvest measured in pine needles (a), stem (b), roots (c) and rhizosphere soil (d). Plants were grown in a chamber (circle red) or under outdoor conditions (triangle yellow) through 19 (plants A, C, D and N), 28 (B and M), 34 (G, H, I and L) and 39 days (E, F, J and K). All data were decay-corrected.

As intended, the day temperatures were warmer in the chamber than the outdoor day temperatures. However, the night temperatures did not turn out as planned. We set the chamber overnight temperatures based on the average for the period 1985–2015 (outdoor). However, during our experimental period, the nights were on average warmer than the average and warmer than the chamber treatment. In consequence, the night chamber temperatures were therefore slightly (6 to 1°C) colder than outside. None-the-less, the effect of higher daytime temperature in the chambers on the quantitative P uptake from P-labelled hydroxylapatite was still positive when compared to outside, as clearly supported by the (bio)image. This suggests that the higher temperature during the photosynthetic period had a bigger effect on P uptake than the nights.

Seedling growth responses to temperature treatments can differ aboveground and belowground. For chamber-grown *Picea abies*, it was found that root growth was decreased in colder grown seedlings, while shoot growth was decreased in warmer grown seedlings (Lahti et al., 2005). In a field experiment with warming, Nissinen et al. (2020) found that *Picea abies* growth (height and biomass) responded positively through three growing seasons, but *Pinus sylvestris* had an even larger positive response to warming than *Picea abies*. We did not confirm, based on our results, if the chamber effect was due mainly to faster uptake in the plant root or shoot, or to a more rapid release of phosphate from the apatite in the experiment. These complex processes are likely happening at different rates. Dissolution of apatite is likely controlled by soil moisture, temperature and acidity (e.g. pk_H 12.8 and pk_{H2O} 15.8 kmol m^{-2} s^{-1} values are used in the PROFILE model; Casetou-Gustafson et al., 2019), while the uptake rate by the plant root is set by the number and activity of transporter proteins in the plant root, which are downregulated at increasing pH, but also respond to the P status of the plant plasmalemma (Smith, 2002).

The plants were inoculated with spruce forest soil from Sweden containing (unspecified) ECM spores (as we identified ECM sporocarps in the forest); therefore, we assume

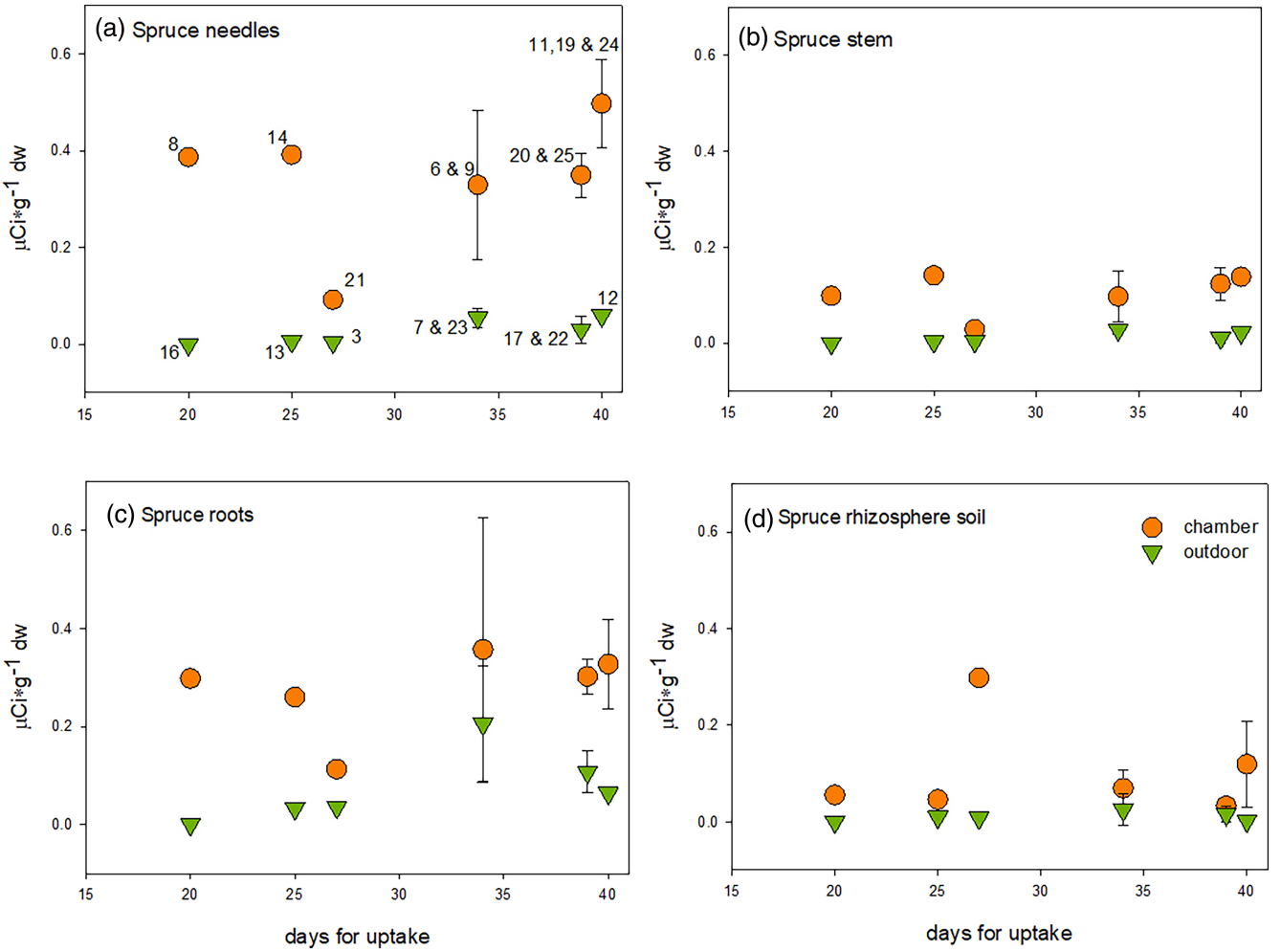

FIGURE 4 Absolute radioactivity as micro-Curie per gram dry weight (dw) measured in spruce needles (a), stem (b), roots (c) and rhizosphere soil (d). Plants were grown in chamber (circle orange; warm) or under outdoor conditions (triangle green; cold) through 20 (plants nr. 8 and 16), 25 (nr. 13 and 14), 27 (nr. 3 and 21), 34 (nr. 6, 7, 9 and 23), 39 (nr. 17, 20, 22 and 25) and 40 days (nr. 11, 12, 19 and 24).

that the experimental plants had developed ECM symbiosis. Indeed, radioactively labelled fruiting bodies of (unidentified) fungi (both in (bio)images and LSC analysis) were observed in several rhizotrons (data not presented). Investigations using non-radioactive apatite have shown that the ECM in pine forest benefit in growth from the apatite (Almeida et al., 2019; Rosenstock et al., 2016; Smits et al., 2014; Wallander, 2000; Wallander & Thelin, 2008; Wallander et al., 2003). Schreider et al. (2022) found that P uptake from P-labelled hydroxylapatite (^{33}P labelled) happened exclusively when *Populus x canescens* plants were inoculated with the ECM component *Paxillus involutus*. Considering these earlier results, we suggest that the uptake we measured in the needles and stem of pine and spruce in our experiment (Figures 3 and 4) was mediated by the ECM interaction with apatite. Unfortunately, for reasons of safety, we did not measure labelling of ECM in our experiment.

The soils in the experiment were organic to avoid any potential adsorption of the apatite and phosphate to minerals and clays. Swedish forest soils commonly have an organic topsoil layer more than 7 cm thick (in 94% of all soils; SLU Mark och Miljö, 2023). Furthermore, organic soils (Histosols) are common in Sweden, especially in mid-Sweden near the field station (SLU Mark och Miljö, 2023). Therefore, our experiment was carried out with soil representative for Swedish conditions, particularly for the soil layer with most fine roots.

We did not anticipate leaching of apatite, as it is quite insoluble, and we kept the plants and soil relatively dry during the incubations. The leaching tests supported our assumption that neither ^{33}P-apatite nor P or Ca leached from the experimental soil volume. Therefore, we consider the setup a closed system.

As our experiment only used pure hydroxylapatite (Figure S1), we cannot yet demonstrate that apatite gained from mining products—which will contain a mixture of various types of apatite, such as fluorine- and chlorine-endmembers, may be accessed equally well by plants.

Furthermore, our soil was highly organic (sphagnum) and 'plant oriented' ('null-erde') but contained no clays; therefore, we cannot assure that apatite amendment to more natural soils in forests is as labile as found here, as chemical adsorption might happen at the clay surfaces.

5 | CONCLUSIONS

Our hypothesis was confirmed; the two conifer species, which are very important in forestry in Scandinavia, do utilize P from apatite when this is amended in the soil. The results suggest that warmer future daytime temperatures will lead to an increased tree uptake of soil apatite-P. Apatite fertilization of managed spruce and pine forests is therefore a feasible option as it will indeed lead to enhanced plant P uptake and thus the likelihood of increasing wood production.

AUTHOR CONTRIBUTIONS

Louise Rütting: Writing – original draft; methodology; supervision; resources; conceptualization; formal analysis; writing – review and editing; visualization; funding acquisition. **Diana Hofmann:** Conceptualization; methodology; writing – review and editing; formal analysis; supervision; visualization; funding acquisition; resources. **Thomas Pütz:** Conceptualization; methodology; writing – review and editing; formal analysis; supervision; resources; funding acquisition; visualization. **Matthias Konrad-Schmolke:** Conceptualization; writing – review and editing; formal analysis; visualization; funding acquisition; methodology; supervision; resources. **Roland Bol:** Conceptualization; writing – review and editing; formal analysis; resources; supervision; methodology; funding acquisition; visualization.

ACKNOWLEDGEMENTS

Simon Horn, Ursula Paffen, Stephan Köppchen and Philipp Meulendick are thanked for lab assistance and/or safety assistance. ZEA-3 made the elemental analysis of start soil and plant. Formas 2017-00423. The faculty of Science at University of Gothenburg sabbatical program supported Louise C. Andresen (Louise Rütting) and this research. Open Access funding enabled and organized by Projekt DEAL.

DATA AVAILABILITY STATEMENT

The data that support the findings of this study are available from the corresponding author upon reasonable request.

ORCID

Louise Rütting https://orcid.org/0000-0002-4890-889X

REFERENCES

Adediran, G. A., Kielman-Schmitt, M., Kooijman, E., & Gustafsson, J. P. (2022). Significance of phosphorus inclusions and discrete micron-sized grains of apatite in postglacial forest soils. *European Journal of Soil Science*, *73*, e13310.

Adhikari, T., Kundu, S., Meena, V., & Rao, A. S. (2014). Utilization of nano rock phosphate by maize (*Zea mays* L.) crop in a vertisol of Central India. *Journal of Agricultural Science and Technology A*, *4*, 384–394.

Akselsson, C., Westling, O., Alveteg, M., Thelin, G., Fransson, A. M., & Hellsten, S. (2008). The influence of N load and harvest intensity on the risk of P limitation in Swedish forest soils. *Science of the Total Environment*, *404*, 282–289.

Almeida, J. P., Rosenstock, N. P., Forsmark, B., Bergh, J., & Wallander, H. (2019). Ectomycorrhizal community composition and function in a spruce forest transitioning between nitrogen and phosphorus limitation. *Fungal Ecology*, *40*, 4020–4031.

Andresen, L. C., Michelsen, A., Jonasson, S., Beier, C., & Ambus, P. (2009). Glycine uptake in heath plants and soil microbes responds to elevated temperature, CO_2 and drought. *Acta Oecologica*, *35*(6), 786–796.

Basirirad, R. (2000). Research review kinetics of nutrient uptake by roots: Responses to global change. *The New Phytologist*, *147*, 155–169.

Bauke, S. L., Landl, M., Koch, M., Hofmann, D., Nagel, K. A., Siebers, N., Schnepf, A., & Amelung, W. (2017). Macropore effects on phosphorus acquisition by wheat roots – A rhizotron study. *Plant and Soil*, *416*, 67–82. https://doi.org/10.1007/s11104-017-3194-0

Becquer, A., Guerrero-Galán, C., Eibensteiner, J. L., Houdinet, G., Bücking, H., Zimmermann, S. D., & Garcia, K. (2019). Molecular Physiology and Biotechnology of Trees. In *Advances in Botanical Research*. Elsevier. https://doi.org/10.1016/bs.abr.2018.11.003.

Bloom, A. J., Stuart Chapin, F., III, & Mooney, H. A. (1985). Resource limitation in plants-an economic analogy. *Annual Review of Ecology and Systematics*, *16*, 16363–16392.

Bucking, H., & Heyser, W. (2003). Uptake and transfer of nutrients in ectomycorrhizal associations: Interactions between photosynthesis and phosphate nutrition. *Mycorrhiza*, *13*(2), 59–68.

Cairney, J. W. G. (2011). Ectomycorrhizal fungi: The symbiotic route to the root for phosphorus in forest soils. *Plant and Soil*, *344*(1–2), 51–71.

Casetou-Gustafson, S., Akselsson, C., Hillier, S., & Olsson, B. A. (2019). The importance of mineral determinations to PROFILE base cation weathering release rates: A case study. *Biogeosciences*, *16*, 1903–1920.

Clarholm, M., & Rosengren-Brinck, U. (1995). Phosphorus and nitrogen fertilization of a Norway spruce forest - effects on needle concentrations and acid phosphatase activity in the humus layer. *Plant and Soil*, *175*, 239–249.

Colin, Y., Turpault, M. P., Fauchery, L., Buée, M., & Uroz, S. (2021). Forest plant cover and mineral type determine the diversity and composition of mineral-colonizing fungal communities. *European Journal of Soil Biology*, *105*, 103334.

Cordell, D., & White, S. (2011). Peak phosphorus: Clarifying the key issues of a vigorous debate about long-term phosphorus security. *Sustainability*, *3*(10), 2027–2049.

Cronan, C. S. (2018). *Ecosystem biogeochemistry - element cycling in the forest landscape*. Springer.

Domevscik, M., Wallertz, K., & Hjelm, K. (2024). Effect of drought and pine weevil damage on mechanically protected Norway spruce seedlings. *Forest Ecology and Management*, *566*, 122053.

Drott, A., Anderson, S., & Eriksson, H. (2019). *Regler och rekommendationer för skogsbränsleuttag och kompensationsåtgärder*. Skogsstyrelsen.

EAGE News. (2017). EAGE to partner in EU project for sustainable mineral exploration. *First Break*, *I35*, 3–4.

Faradji, F., & de Boer, M. (2016). How the great phosphorus shortage could leave us all hungry. *The Conversation* SSUU.

Guidry, M. W., & Mackenzie, F. T. (2000). Apatite weathering and the Phanerozoic phosphorus cycle. *Geology*, *28*(6), 31–634.

Hasegawa, S., Macdonald, C. A., & Power, S. A. (2016). Elevated carbon dioxide increases soil nitrogen and phosphorus availability in a phosphorus-limited *Eucalyptus* woodland. *Global Change Biology*, *22*, 1628–1643. https://doi.org/10.1111/gcb.13147

He, H., Jansson, P.-E., & Gärdenäs, A. I. (2021). CoupModel (v6.0): An ecosystem model for coupled phosphorus, nitrogen, and carbon dynamics – Evaluated against empirical data from a climatic and fertility gradient in Sweden. *Geoscientific Model Development*, *14*(2), 735–761.

Hofmann, D., Thiele, B., Rahmati, M., Siebers, M., Schütz, V., Jeong, S., Cui, J., Bigler, L., Held, F., Wu, B., Babic, N., Kovacic, F., Hamacher, J., Hölzl, G., Dörmann, P., & Schulz, M. (2023). Implications of below ground Allelopathic interactions of Camelina sativa and microorganisms for phosphate availability and habitat maintenance. *Plants*, *12*(15), 2815. https://doi.org/10.3390/plants12152815

Hou, E., Chen, C., Luo, Y., Zhou, G., Kuang, Y., Zhang, Y., Heenan, M., Lu, X., & Wen, D. (2018). Effects of climate on soil phosphorus cycle and availability in natural terrestrial ecosystems. *Global Change Biology*, *24*, 3344–3356.

Iversen, C. M., Latimer, J., Brice, D. J., Childs, J., Stel, H. M. V., Defrenne, C. E., Graham, J., Griffiths, N. A., Malhotra, A., Norby, R. J., Oleheiser, K. C., Phillips, J. R., Salmon, V. G., Sebestyen, S. D., Yang, X., & Hanson, P. J. (2023). Whole-ecosystem warming increases plant-available nitrogen and phosphorus in an Ombrotrophic bog. *Ecosystems*, *26*, 86–113.

Jacobsen, S., Pettersson, F., Högbom, L., & Sikström, U. (2005). *Skogsgödsling - en handledning från Skogforsk*. Stiftelsen Skogsbrukets Forskningsinstitut.

Koch, M., Schiedung, H., Siebers, N., McGovern, S., Hofmann, D., Vereecken, H., & Amelung, W. (2019). Quantitative imaging of ^{33}P in plant materials using ^{14}C polymer references. *Analytical and Bioanalytical Chemistry*, *411*, 1253–1260.

Kottegoda, N., Sandaruwan, C., Priyadarshana, G., Siriwardhana, A., Rathnayake, U. A., Berugoda Arachchige, D. M., Kumarasinghe, A. R., Dahanayake, D., Karunaratne, V., & Amaratunga, G. A. (2017). Urea-hydroxyapatite nanohybrids for slow release of nitrogen. *ACS Nano*, *11*(2), 1214–1221.

Kumar, J., & Atri, N. S. (2017). Studies on Ectomycorrhiza: An appraisal. *The Botanical Review*, *84*(2), 108–155.

Lahti, M., Aphalo, P. J., Finér, L., Ryyppö, A., Lehto, T., & Mannerkoski, H. (2005). Effects of soil temperature on shoot and root growth and nutrient uptake of 5-year-old Norway spruce seedlings. *Tree Physiology*, *25*, 115–122.

Linder, S. (1995). Foliar analysis for detecting and correcting nutrient imbalances in Norway spruce. *Ecological Bulletins*, *44*, 178–190.

Liu, R., & Lal, R. (2014). Synthetic apatite nanoparticles as a phosphorus fertilizer for soybean (Glycine max). *Scientific Reports*, *4*(1), 5686.

Magnusson, T. (2015). *Skogsbruk - mark och vatten*. Skogsstyrelssen.

Nair, R., Varghese, S. H., Nair, B. G., Maekawa, T., Yoshida, Y., & Kumar, D. S. (2010). Nanoparticulate material delivery to plants. *Plant Science*, *179*(3), 154–163.

Nissinen, K., Virjamo, V., Kilpeläinen, A., Ikonen, V.-P., Pikkarainen, L., Ärväs, I.-L., Kirsikka-aho, S., Peltonen, A., Sobuj, N., Sivadasan, U., Zhou, X., Ge, Z.-M., Salminen, T., Julkunen-Tiitto, R., & Peltola, H. (2020). Growth responses of boreal scots pine, Norway spruce and silver birch seedlings to simulated climate warming over three growing seasons in a controlled field experiment. *Forests*, *2020*(11), 943. https://doi.org/10.3390/f11090943

Pendall, E., Bridgham, S., Hanson, P. J., Hungate, B., Kicklighter, D. W., Johnson, D. W., Law, B. E., Luo, Y., Megonigal, J. P., Olsrud, M., Ryan, M. G., & Wan, S. (2004). Below-ground process responses to elevated CO_2 and temperature: A discussion of observations, measurement methods, and models. *The New Phytologist*, *162*, 311–322.

Rakovan, J., & Scovil, J. A. (2021). Apatite and the apatite supergroup. *Rocks & Minerals*, *96*(1), 13–19.

Rennenberg, H., & Herschbach, C. (2013). Phosphorus nutrition of woody plants: Many questions - few answers. *Plant Biology (Stuttgart, Germany)*, *15*(5), 785–788.

Rico, C. M., Majumdar, S., Duarte-Gardea, M., Peralta-Videa, J. R., & Gardea-Torresdey, J. L. (2011). Interaction of nanoparticles with edible plants and their possible implications in the food chain. *Journal of Agricultural and Food Chemistry*, *59*(8), 3485–3498.

Roberts, K., Defforey, D., Turner, B. L., Condron, L. M., Peek, S., Silva, S., Kendall, C., & Paytan, A. (2015). Oxygen isotopes of phosphate and soil phosphorus cycling across a 6500 year chronosequence under lowland temperate rainforest. *Geoderma*, *257–258*, 14–21.

Roeder, P. L., MacArthur, D., Ma, X. P., Palmer, G. R., & Mariano, A. N. (1987). Cathodoluminescence and microprobe study of rare-earth elements in apatite. *American Mineralogist*, *72*(7–8), 801–811.

Rosenstock, N. P., Berner, C., Smits, M. M., Krám, P., & Wallander, H. (2016). The role of phosphorus, magnesium and potassium availability in soil fungal exploration of mineral nutrient sources in Norway spruce forests. *The New Phytologist*, *211*, 542–553. https://doi.org/10.1111/nph.13928

Schlesinger, W. H., & Bernhardt, E. S. (2020). *Biogeochemistry* (4th ed.). Academic Press.

Schreider, K., Hofmann, D., Boy, J., Andrino, A., Figueiredo, A. F., Sauheitl, L., & Guggenberger, G. (2022). Mycorrhizal mediated partitioning of phosphorus: Ectomycorrhizal (*Populus* × *canescens* × *Paxillus involutus*) potential to exploit simultaneously organic and mineral phosphorus sources. *Frontiers in Soil Science*, *2*, 865517.

Skogsstyrelsen. (2015). Föreskrifter om ändring i Skogsstyrelsens föreskrifter (SKSFS 2011:7) och allmänna råd till skogsvårdslagen.

Högberg, P., Larsson, S., Lundmark, T., Moen, J., Nilsson, U., & Nordin, A. (2014). Effekter av kvävegödsling på skogsmark - Kunskapssammanställning utförd av SLU på begäran av Skogsstyrelsen, 1857.

SLU Forest Statistics; Petersson, H. (2023). Institutionen för skoglig resurshushållning.

SLU Mark och Miljö, Institutionen för Mark och Miljö (2023) www.slu.se/institutioner/mark-miljo/miljoanalys/markinfo/kartor/.

Smeck, N. E. (1985). Phosphorus dynamics in soils and landscapes. *Geoderma*, *36*, 36185–36199.

Smith, A. W. (2002). The phosphate uptake mechanism. *Plant and Soil*, *245*(1), 105–114.

Smits, M. M., Bonneville, S., Benning, L. G., Banwart, S. A., & Leake, J. R. (2012). Plant-driven weathering of apatite – The role of an ectomycorrhizal fungus. *Geobiology*, *10*(5), 445–456.

Smits, M. M., Johansson, L., & Wallander, H. (2014). Soil fungi appear to have a retarding rather than a stimulating role on soil apatite weath. *Plant and Soil*, *385*, 217–228.

Solanki, P., Bhargava, A., Chhipa, H., Jain, N., & Panwar, J. (2015). Nano-fertilizers and their smart delivery system. In *Nanotechnologies in food and agriculture* (pp. 81–101). Springer.

Ståhl, P. H., & Bergh, J. (2013). Produktionshöjande åtgärder, *Skogsstyrelsen*.

Taşkın, M. B., Şahin, Ö., Taskin, H., Atakol, O., Inal, A., & Gunes, A. (2018). Effect of synthetic nano-hydroxyapatite as an alternative phosphorus source on growth and phosphorus nutrition of lettuce (Lactuca sativa L.) plant. *Journal of Plant Nutrition*, *41*(9), 1148–1154.

Tuyishime, J. R. M., Adediran, G. A., Olsson, B. A., Spohn, M., Hillier, S., Klysubun, W., & Gustafsson, J. P. (2022). Phosphorus abundance and speciation in acid forest Podzols – Effect of post-glacial weathering. *Geoderma*, *406*, 115500.

Wallander, H. (2000). Uptake of P from apatite by *Pinus sylvestris* seedlings colonised by different ectomycorrhizal fungi. *Plant and Soil*, *218*, 249–256.

Wallander, H., Mahmood, S., Hagerberg, D., Johansson, L., & Pallon, J. (2003). Elemental composition of ectomycorrhizal mycelia identifed by PCR-RFLP analysis and grown in contact with apatite or wood ash in forest soil. *FEMS Microbiology Ecology*, *44*, 57–65.

Wallander, H., & Thelin, G. (2008). The stimulating effect of apatite on ectomycorrhizal growth diminishes after PK fertilization. *Soil Biology and Biochemistry*, *40*(10), 2517–2522.

Weirauch, C., & Opp, C. (2018). Ecologically relevant phosphorus pools in soils and their dynamics: The story so far. *Geoderma*, *325*, 183–194.

Wolff, J., Hofmann, D., Amelung, W., Lewandowski, H., Kaiser, K., & Bol, R. (2018). Rapid wet chemical synthesis for ^{33}P-labelled hydroxyapatite – An approach for environmental research. *Applied Geochemistry*, *97*, 97181–97186.

Wolff, J., Hofmann, D., Maximilian, K., Bol, R., Schnepf, A., & Amelung, W. (2020). Bioavailability and -accessibility of subsoil allocated ^{33}P-labelled hydroxyapatite to wheat under different moisture supply. *Scientific Reports*, *10*, 17140.

Xu, B., Kou, G., Etschmann, B., Liu, D., & Brugger, J. (2020). Spectroscopic, Raman, EMPA, micro-XRF and micro-XANES analyses of sulphur concentration and oxidation state of natural apatite crystals. *Crystals*, *10*(11), 1032.

Yu, L., Caldararu, S., Ahrens, B., Wutzler, T., Schrumpf, M., Helfenstein, J., Pistocchi, C., & Zaehle, S. (2023). Improved representation of phosphorus exchange on soil mineral surfaces reduces estimates of phosphorus limitation in temperate forest ecosystems. *Biogeosciences*, *20*, 57–73.

Zhao, X., Tian, Q., Michelsen, A., Lu, M., Ren, B., Huang, L., & Zhao, R. (2023). The effect of experimental warming on fine root functional traits of woody plants: Data synthesis. *Science of the Total Environment*, *894*, 165003.

SUPPORTING INFORMATION

Additional supporting information can be found online in the Supporting Information section at the end of this article.

How to cite this article: Rütting, L., Hofmann, D., Pütz, T., Konrad-Schmolke, M., & Bol, R. (2024). Spruce and pine utilization of phosphorus in soil amended with ^{33}P-labelled hydroxylapatite. *European Journal of Soil Science*, *75*(5), e13587. https://doi.org/10.1111/ejss.13587